A classical dynamics study of the anisotropic interactions in NNO–Ar and NNO–Kr systems: Comparison with transport and relaxation data

Marc A. ter Horst[a] and Cynthia J. Jameson
Department of Chemistry M/C-111, University of Illinois at Chicago, 845 W. Taylor, Chicago, Illinoi 60607-7061

(Received 6 July 1998; accepted 10 September 1998)

Classical trajectory calculations were carried out on potential-energy surfaces (PES) that have been proposed for NNO–Ar and NNO–Kr. Two types of cross sections involving the molecular rotational angular momentum vector, $\sigma_{\theta,2}$ and σ_J, that are particularly sensitive to the anisotropy of the potential function are compared with new experimental data from our spin-relaxation measurements (see the preceding paper). There is very good agreement with one cross section, $\sigma_{\theta,2}$, but less favorable agreement with σ_J. Spectroscopic data for the van der Waals complexes are compared with the values calculated from the surfaces using quantum diffusion Monte Carlo simulations. © *1998 American Institute of Physics.* [S0021-9606(98)01147-7]

INTRODUCTION

van der Waals complexes of NNO with various molecules have been observed. Molecular beam electric resonance spectroscopy first showed that the structure of the NNO–Ar complex is T-shaped.[1] High-resolution infrared (IR) spectroscopy of jet cooled systems have provided structural information for: NNO–CO_2,[2] NNO–CO,[3,4] NNO–N_2,[5] NNO–HCl,[6] NNO–Ar,[7,8] other NNO–rare gas,[9] and $(NNO)_2$.[10,11] Pulsed Fourier transform microwave spectroscopy of a number of isotopomers of NNO–HCl provided good comparisons with *ab initio* calculations at the Moller–Plesset second-order (MP2) level,[12] and the nuclear quadrupole hyperfine structure due to both nitrogen nuclei in NNO–Ar and in NNO–CO2 is found to support the utility of quadrupolar nuclei in extracting geometrical information in such complexes.[13,14] Other spectroscopic data such as the mean-square torque have been measured for NNO–Ar and NNO–Kr,[15,16] and recently also for NNO–Xe and NNO–CO_2,[17] and for NNO–SF_6.[18] Furthermore, rotational relaxation rates for the $J=0-1$ transitions of $^{15}N^{15}NO$ upon collisions with NNO, N_2, Ar, Kr, and Xe have been determined by pulsed microwave time domain spectroscopy, providing the pressure dependence of the population and coherence decay rates $1/T_1$ and $1/T_2$.[19] These relaxation rates depend on the anisotropy of the potential. A direct determination of the cross sections $\sigma_{\theta,2}$, for reorientation of the molecular rotational angular momentum vector, has recently become available (see the preceding paper, Ref. 20) and the other cross sections σ_J had previously been reported for the NNO molecule in collisions with these molecules.[21] In previous work by McCourt and co-workers, the magnitude and temperature dependence of the cross sections $\sigma_{\theta,2}$ and σ_J have been shown to be very sensitive to the anisotropy of the potential surface of H_2 interacting with He, Ne, and Ar,[22–24] and of N_2–Ar.[25] Our classical trajectory studies on CO_2–Ar,[26] and N_2–Kr[27,28] have shown that these cross sections can discriminate between potential surfaces that otherwise perform equally well in their predictions of other thermophysical properties.

With the increasing interest in the complexes involving the NNO molecule, it is useful to examine the potential surfaces that have been proposed. Of the NNO–X pairs, potential surfaces have been proposed for NNO–Ar and NNO–Kr. In this paper, we examine these surfaces using classical trajectory calculations to evaluate the full set of effective cross sections relevant to gas-phase properties. We use the cross sections associated with the thermophysical properties to calculate the mixture viscosity and diffusion coefficient to compare with the values measured for the NNO–Ar, and NNO–Kr mixtures, and we compare the cross sections for changes in the molecular rotational angular momentum vector, $\sigma_{\theta,2}$ and σ_J, with the values that are directly derived from the NMR relaxation measurements. In addition, we consider the ability of these surfaces to predict the structures of the van der Waals complexes by comparing the average values of the rotational constants obtained from these surfaces using the quantum diffusion Monte Carlo (QDMC) method.

POTENTIAL FUNCTIONS FOR NNO–Ar AND NNO–Kr

In this paper we consider the NNO–Ar and NNO–Kr surfaces proposed by Berreby and Dayan, which have the following form:[15]

$$V(R,\theta)=4\epsilon\{(\sigma/R)^{12}[1+\delta P_2(\cos\theta)] - (\sigma/R)^6[1+\gamma P_2(\cos\theta)]\}, \quad (1)$$

where ϵ and σ were determined from the usual simple combining rules using isotropic values for the pure systems. The anisotropy of polarizability γ of the linear rotor was used to include an attractive anisotropy while the repulsive anisotropy was controlled by δ which was determined from fits to experimental values of the mean-square torque. Note that

[a]Present address: Department of Chemistry, Northwestern University, Evanston, IL 60208-3113.

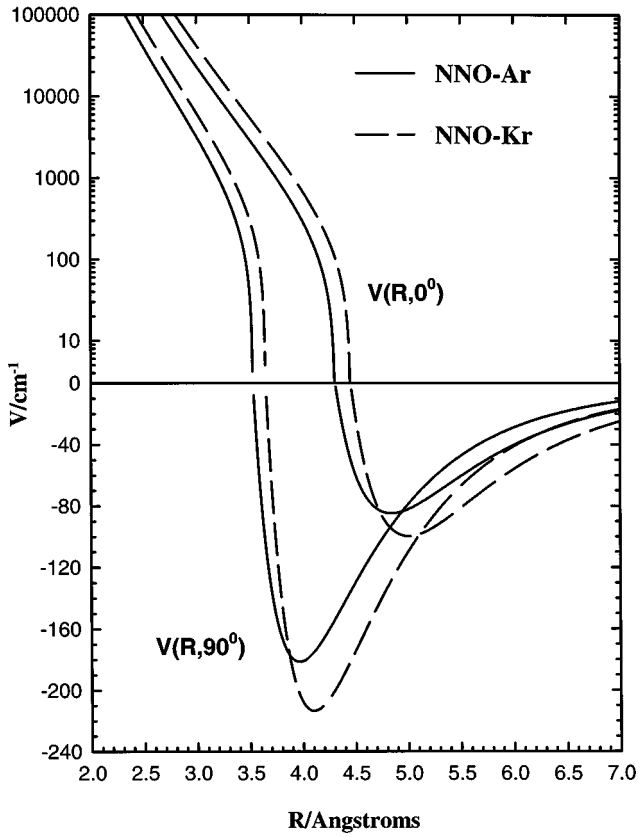

FIG. 1. Cuts at $\theta = 90°$ and 0° of the NNO–Ar and NNO–Kr surfaces used in this work. The functional form is given in Eq. (1) with parameters from Ref. 15.

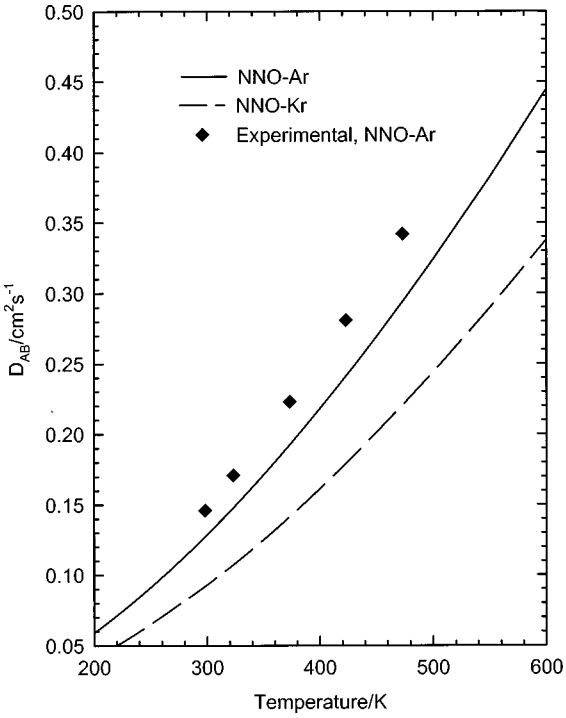

FIG. 2. Temperature dependence of the diffusion coefficient in NNO–Ar and NNO–Kr calculated using the BDAr and the BDKr surfaces, compared with the data from Ref. 33.

only the first two terms of even symmetry have been retained. This type of symmetry is a reasonable first approximation to the true surface when the odd terms in the Legendre expansion are small. Indeed, molecular beam electric resonance study of the NNO–Ar van der Waals molecule reveals an equilibrium structure with an angle very nearly 90° (87.4±1.5°), with the argon atom tilted slightly toward the oxygen atom.[1] Berreby and Dayan note that P_0 and P_2 symmetry is sufficient to fit the data,[15] suggesting that $\langle C^2 \rangle$ may not be extremely sensitive to individual contributions of the Legendre expansion. Nevertheless, the lack of $P_1(\cos\theta)$ symmetry in the proposed NNO–X potentials is an inherent flaw. Cuts of these surfaces are shown in Fig. 1. The characteristic parameters of the functions are in Table I.

RESULTS AND DISCUSSION

Classical trajectory results

Classical trajectory calculations were carried out for a full set of effective cross sections relevant to the bulk gas phenomena,[29,30] following the same procedures used for the N_2–Kr[27,28] and CO_2–Ar systems.[26] The thermally averaged cross sections for the NNO–Ar surface (BDAr) and those for the NNO–Kr surface (BDKr) at four temperatures from 200 to 800 K are reported in the Ph.D. thesis of MAtH (Ref. 31) and are not reproduced here. The agreement between the cross sections related by time reversal symmetry was better here than that found for similar calculations carried out for the CO_2–Ar system.[26] Experimental values for the diffusion coefficient are available only for the NNO–Ar system. From their viscosity measurements,[32] Kestin and Ro determined values of the diffusion coefficient for NNO–Ar using the extended law of corresponding states.[33] Figure 2 compares the diffusion coefficients calculated from the thermally averaged cross sections with the results of Kestin and Ro.[33] The results of the NNO–Kr calculations are also included here for comparison. Although the general temperature dependence is adequate, the calculated values underestimate the magnitude. In Fig. 3 the agreement with the essentially linear molefraction dependence of the experimental viscosity data[32] is poor, with the mole fraction dependence exaggerated. The calculated results lie beyond the error bars which are ±0.3%.[32]

TABLE I. Characteristics of the Berreby–Dayan surfaces for NNO–Ar and NNO–Kr.

	$\epsilon(90°)/k_B$, K	$R_m(90°)$, Å	$\sigma(90°)$, Å	$\epsilon(0°)/k_B$, K	$R_m(0°)$, Å	$\sigma(0°)$, Å
BDAr	260.9	3.966	3.533	121.9	4.844	4.315
BDKr	307.0	4.101	3.654	143.5	5.008	4.462

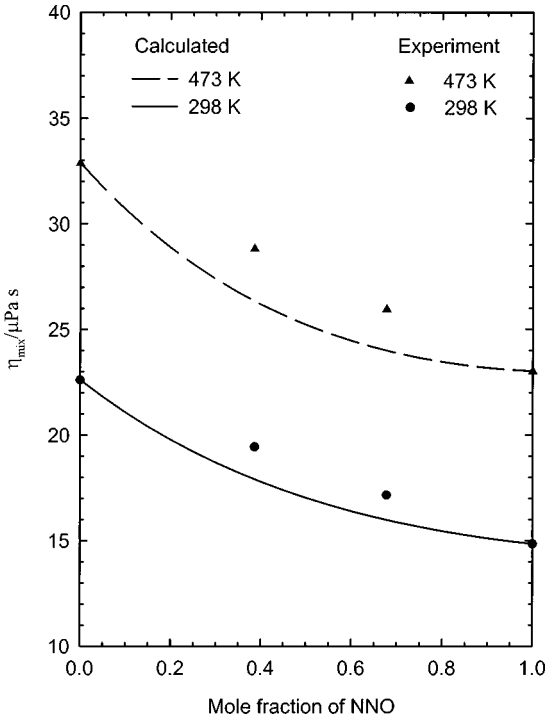

FIG. 3. Mole fraction dependence of the mixture viscosity in NNO–Ar at two temperatures, calculated using the BDAr surface, compared with data from Ref. 32.

Mean-square torque and NMR cross sections for NNO–Ar and NNO–Kr

The mean-square torque $\langle C^2 \rangle$ is related to the second and fourth spectral moments $M(2)$ and $M(4)$ of the absorption profile of an IR absorption band[34]

$$\langle C^2 \rangle = [M(4) - 2M^2(2)]/4B^2, \tag{2}$$

where B is the rotational constant. In the binary collision limit, Armstrong *et al.*[35] have shown that $\langle C^2 \rangle$ may be written in terms of an integral over the angular derivative of the interaction potential, $V(R,\theta)$

$$\langle C^2 \rangle / \rho_X = 2\pi N_0 \int \int (\partial V(R,\theta)/\partial\theta)^2 \times \exp[-V(R,\theta)/k_B T] R^2 \sin\theta d\theta dR, \tag{3}$$

where ρ_X is the number density of the perturbing gas in the NNO–X system in which the NNO IR bands are observed. From spectral moments of infrared vibrational rotational bands, mean-square torques have been measured for NNO mixed with Ar and Kr. These appear to be a linear function of the density up to 250 amagat. We have calculated the mean-square torque using Eq. (3) for the surfaces used here and compare them with the experimental results[15,16] in Table II. The agreement is good, which should be expected since the value of the parameter δ in the potential functions given by Eq. (1) was adjusted to the slope $\langle C^2 \rangle / \rho$ at 300 K. Dreyfus *et al.* have calculated the mean-square torque for NNO in Ar using potential surfaces based on electron gas calculations, but did not provide a functional form.[36] They found a global minimum at about 4.0 Å, depending on the arbitrary choice of a parameter in the dispersion energy. Their results show no better agreement with the experimental temperature dependence than the Berreby–Dayan function that we have used here. It is interesting to note that the experimental $\langle C^2 \rangle / \rho$ for NNO–Ar show a nonlinear behavior with temperature, exhibiting a minimum at around 223 K. Given the quoted experimental error estimates, there is some uncertainty about whether the minimum is real or not. We do not find a minimum in the calculated values of $\langle C^2 \rangle / \rho$ for NNO–Ar using this potential. However, using a modified potential with a somewhat deeper well and shorter $R_{\min}$ does result in a minimum in the calculated mean-square torque. For NNO–Kr we do find a minimum in the mean-square torque calculated using the Berreby–Dayan potential, shown in Table II. It should be expected that the general temperature dependence of the mean-square torque would be of this nature, provided data is taken over a wide enough temperature range.

TABLE II. Mean-square torque of NNO in Ar and Kr, $\langle C^2 \rangle / \rho$, cm^{-2}/amagat.

T, K	Calculated using the BDAr surface, this work[a]	NNO–Ar Expt.[b,c]	Calculated using the BDKr surface, this work[a]	NNO–Kr Expt.[b]
155	483	550±100	993	
173	488	510±100	953	
223	566	480±100	953	
273	647	640±100	1059	
300	693	790±100	1106	1090±100
323	733	760±100	1173	

[a]From integration according to Eq. (3).
[b]From Ref. 15.
[c]From Ref. 16.

Measurements of relaxation times for both isotopic species $^{14}N^{14}NO$ and $^{15}N^{15}NO$ species in mixtures of NNO–Ar and NNO–Kr provide two independent sources of information. The first comes from the dominance of the quadrupolar mechanism for ^{14}N of the end nitrogen[20,31] and the second comes from the dominance of the spin-rotation mechanism for the ^{15}N nuclei.[21] In these cases, the measured relaxation times lead directly to the cross sections σ_J and $\sigma_{\theta,2}$ for the NNO–X systems. Experimental cross sections are available for X=Ar, Kr, CH_4, CF_4, SF_6, N_2, CO, CO_2, NNO, and HCl. The values of the cross sections calculated here for NNO–Ar and NNO–Kr are compared with the experimental results in Figs. 4 and 5. The temperature dependence of $\sigma_{\theta,2}$ and σ_J are well reproduced. Although the surfaces do not reproduce the magnitude of the σ_J values, remarkably good agreement with experiment is obtained for $\sigma_{\theta,2}$ in both NNO–Ar and NNO–Kr systems. The potential surfaces had been adjusted to the experimental mean-square torque $\langle C^2 \rangle$ values. Thus, the excellent ability of these surfaces to predict $\sigma_{\theta,2}(T)$ implies a possible connection between the $\langle C^2 \rangle$ and $\sigma_{\theta,2}$, but not $\langle C^2 \rangle$ with σ_J. From an examination of the contributions to the integral in Eq. (3) from various distances at a given θ, it is clear that the dependence of the mean-square torque on the anisotropy is concentrated in the region of r values within the well. Berreby and Dayan[15] and also Dreyfus *et al.*[36] examined the contributions of the anisotropy

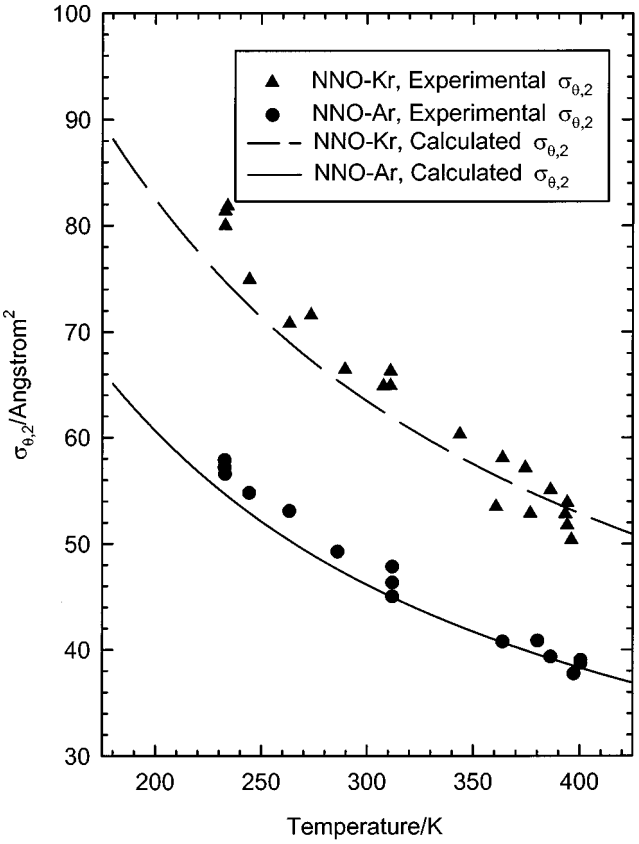

FIG. 4. Temperature dependence of the NMR cross section $\sigma_{\theta,2}$ in NNO–Ar and NNO–Kr calculated using the BDAr and BDKr surfaces, compared with data from Ref. 20.

in the attractive part of the potential to the mean-square torque and found that this was not a major contributor. Their conclusion is that the low repulsive wall plays the main role in determining the mean-square torque. At the same time, there is a general conclusion, resulting from a comparative study of several CO_2–Ar potential surfaces, that both the reorientation cross section $\sigma_{\theta,2}$ and the other NMR cross section, σ_J, depend on the anisotropy of the repulsive wall: Both sets of predicted cross sections are in the same relative order among the six potential surfaces on which classical trajectories had been carried out.[25] In a simple model which qualitatively reproduced the trends in the values of σ_J for nearly a hundred different collision pairs, one of the important factors considered to be determining the magnitudes of σ_J was $(\partial V/\partial\theta_1)$.[37] Detailed studies of the N_2–Ar system by Beneventi *et al.* have shown that the anisotropy of both the low repulsive wall and the upper repulsive wall were important in reproducing σ_J.[25] The present work suggests that while previous studies indicate that both $\sigma_{\theta,2}$ and σ_J depend on $(\partial V/\partial\theta_1)$, the $\sigma_{\theta,2}(T)$ may weight $(\partial V/\partial\theta_1)$ more heavily than does σ_J, resulting in a closer relation between the mean-square torque and $\sigma_{\theta,2}(T)$.

The average properties of the NNO–X complex

Among the techniques that may be applied to the vibrational dynamics of a weakly bound complex is quantum diffusion Monte Carlo (QDMC). Anderson gave the first modern algorithm for simulating the Schrödinger equation as if it were a diffusion process.[38,39] With this we obtain the average rotational constants in the ground vibrational state. Consistent with the rigid geometry assumed for the linear molecule in the calculation of the intermolecular potential energy, we take the molecule to be rigid, as has been done by Buch and others.[40–42] The simulation consists of a number of copies of the system. Each copy is allowed to diffuse via a random walk process and to multiply or disappear with a probability determined by its potential energy. This process is repeated until the distribution of replicas approaches a fluctuating steady state from which the ground-state energy is evaluated. After equilibration, the simulation yields a collection of replicas of the system that have the statistical distribution which approaches the ground-state wave function of the system. Buch has implemented QDMC for two or more interacting molecules, each taken to be rigid, which we adopt here with no changes.[40] This treatment relies on the approximation that the high-frequency intramolecular vibrations are effectively decoupled from the lower frequency intermolecular motions because these two types of motions occur at very different time scales. By eliminating the high-frequency motions the number of variables is decreased and larger time steps may be taken. Rotational constants and all other properties averaged over the zero-point motion were calculated by the method of descendant weighting which provides the means of obtaining expectation values from the distribution gener-

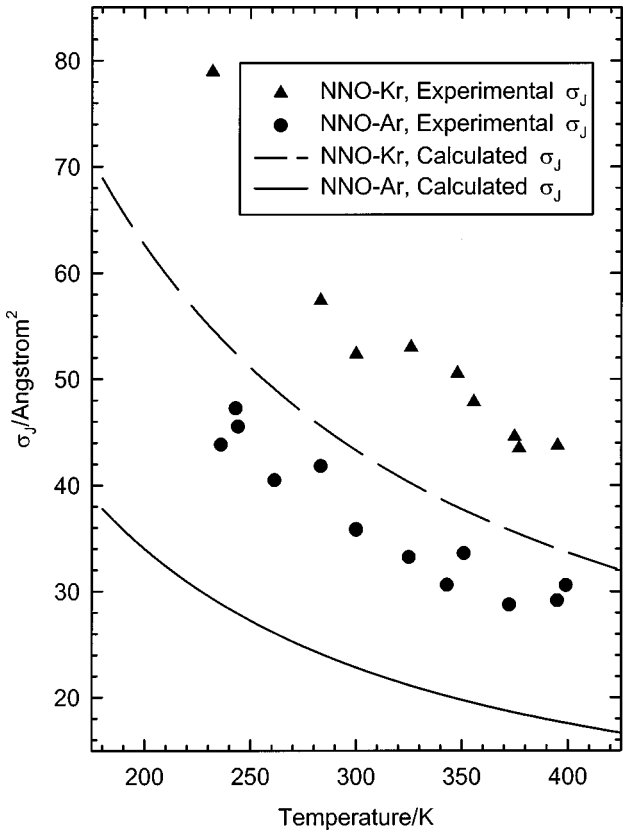

FIG. 5. Temperature dependence of the NMR cross section σ_J in NNO–Ar and NNO–Kr calculated using the BDAr and BDKr surfaces, compared with data from Ref. 21.

TABLE III. Comparison of calculated spectroscopic constants of NNO–Ar with experimental values.

Observable	Calculated using the BDAr potential, this work	Hu *et al.*[a]	Leung *et al.*[d]	Hodge *et al.*[e]	Joyner *et al.*[f]
k_s mdyne/Å	0.016 49[b]	0.0178			0.0194(10)
k_b mdyne·Å	0.010 96[b]	0.0102			0.0213(5)
$\langle R_{cm}\rangle$, Å	4.0663(17)[c]	3.47(2)	3.4686	3.4666	3.460(5)
$\langle \theta_{cm}\rangle$, °	89.96(4)[c]	82.92(1)	82.92 or 97.08	82.92	87.4(15)
A, MHz	12 891.5(37)[c]	12 792.411(36)	12 792.182 23(19)	12 792.157(16)	12 792.203(8)
B, MHz	1463.1(13)[c]	2017.620(21)	2017.116 37(11)	2017.112(8)	2017.486(10)
C, MHz	1313.1(10)[c]	1729.171(23)	1729.587 50(5)	1729.568(7)	1729.223(10)
$\frac{1}{2}(\omega_s+\omega_b)$, cm^{-1}	32.23(19)[c]	$\omega_b=32.2$			
D_0, cm^{-1}	149.08(19)[c]				

[a]Reference 8.
[b]From derivatives of the potential function given by Eq. (1).
[c]From quantum diffusion Monte Carlo solution of the van der Waals vibrational motion. These are averages over the ground-state vibrational wave functions.
[d]Reference 13.
[e]Reference 7.
[f]Reference 1.

ated by QDMC.[43,44] The descendant weighting procedure used to obtain the averages was adopted from Ref. 45. The ground-state energy is obtained from the requirement of stability of the asymptotic average number of replicas. Parameters of the simulations (number of replicas, time step sizes, etc.) are similar to those used previously.[26,46] Using the BDAr and BDKr surfaces to represent the potential energy of NNO–Ar and NNO–Kr, we have obtained from the QDMC simulations the average rotational constants *A,B,C* for the ground vibrational state and the ground-state zero-point energy (and thus the dissociation energy D_0) of these complexes.

These average quantities are compared with the experimental values in Tables III and IV. The shape of the bottom of the potential well provides second derivatives k_s and k_b, the force constants for the stretching and bending of the van der Waals complex. In Table III we see that they do agree reasonably well with the values deduced from the more accurate experimental centrifugal distortion constants in the NNO–Ar complex reported by Hu *et al.*[8] These are consistent with the observed bending frequency of 32.2 cm^{-1} reported by these authors. (Earlier values from Joyner *et al.*[1] do not reproduce this bending frequency.) This is an indication that while the general anisotropy of the PES is reasonably described for the type of averaging that is responsible for the mean-square torque and the temperature dependence of the $\sigma_{\theta,2}$ cross section is concerned, the shape of the bottom of the BDAr potential is also quite good enough to provide good force constants for the van der Waals complex. The BDAr potential, however, fails to give good average values for the structure of the van der Waals complex in the ground vibrational state. The average angle is found very close to 90° because the potential function used does not have odd terms in Legendre functions. The average distance between the center of mass of NNO and the Ar atom is longer by about 0.6 Å compared to experiment. This is reflected also in the average rotational constants obtained; *B* and *C* are too small compared to experiment. A potential surface for the CO_2–Ar system similarly constructed by Berreby and Dayan had been found to have similar weaknesses: $\langle R_{cm}\rangle$ too long, rotational constants *B* and *C* too small, well depth too shallow, while having the shape at the bottom of the well to provide good stretching and bending force constants for the van der Waals complex.[26]

For the NNO–Kr complex there is very limited published data. Although unpublished results by J. Hodge and G. D. Hayman are referred to in Ref. 7, the rotational constants have not been published. The average R_{cm} and θ_{cm} deduced

TABLE IV. Comparison of calculated spectroscopic constants of NNO–Kr with experimental values.

Observable	Calculated using the BDKr potential, this work	Experiment
k_s mdyne/Å	0.018 14[a]	
k_b mdyne·Å	0.012 89[a]	
$\langle R_{cm}\rangle$, Å	4.1835(17)[b]	3.5926[c]
$\langle \theta_{cm}\rangle$, °	89.79(8)[b]	83.02[c]
A, MHz	12 842.8(26)[b]	
B, MHz	1002.9(8)[b]	
C, MHz	929.9(7)[b]	
$\frac{1}{2}(\omega_s+\omega_b)$, cm^{-1}	31.57(8)[b]	
D_0, cm^{-1}	181.83(8)[b]	

[a]From derivatives of the potential function given by Eq. (1).
[b]From quantum diffusion Monte Carlo solution of the van der Waals vibrational motion. These are averages over the ground-state vibrational wave functions.
[c]From Ref. 9.

from the rotational constants have been reported in Ref. 9 and these are compared in Table IV with our QDMC results using the Berreby–Dayan surface. Here too we find that the average distance predicted by the surface is longer by about 0.6 Å than that deduced from the experimental rotational constants. However, the relative magnitudes of zero-point energy found by QDMC simulations for the two complexes appear to be reasonable estimates of $\frac{1}{2}(\omega_s+\omega_b)$, i.e., 32.23(19) cm^{-1} and 31.57(8) cm^{-1}, respectively, for NNO–Ar and NNO–Kr complexes. The global minimum of the Berreby–Dayan potentials are probably too shallow but there are no values for D_0 available for NNO–Ar and NNO–Kr to compare with.

CONCLUSIONS

These are the first calculations of the transport and relaxation cross sections for the NNO–Ar and NNO–Kr systems. The empirical surfaces based on fits to mean-square torque ($\langle C^2\rangle$) data of Berreby and Dayan have been investigated. Neither surface provides adequate prediction of the NMR cross section σ_J although the temperature dependence and the relative magnitudes for NNO–Kr relative to NNO–Ar are well accounted for. On the other hand, the ability of the NNO–Ar and NNO–Kr surfaces to reproduce the magnitudes and the temperature dependence of the NMR cross sections $\sigma_{\theta,2}$ shows promise for further understanding of the dependence of $\sigma_{\theta,2}$ on the PES. For both NNO–Ar and NNO–Kr, the potential surfaces that had been fitted to experimental mean-square torque values give excellent quantitative agreement with the experimental $\sigma_{\theta,2}$. Thus, the present calculations reveal a possible connection, not previously noted, between $\sigma_{\theta,2}$ and $\langle C^2\rangle$. Since $\langle C^2\rangle$ can be written explicitly as an integral over the square of the angular derivative of the potential function, as seen in Eq. (3), this finding suggests that $\sigma_{\theta,2}$ is related to $(\partial V(R,\theta)/\partial\theta)$. That is, the cross section for reorientation of the molecular rotational angular momentum vector of the molecule is strongly dependent on the direction of approach of the collision partner with respect to the NNO molecular axis.

The ability of the surfaces to predict spectroscopic constants and average molecular geometry of the NNO–Ar and NNO–Kr complexes is only fair. As has been found in using their CO_2–Ar surface,[26] the Berreby–Dayan surfaces for NNO–Ar and NNO–Kr are found to have their minimum energy at distances too far out for all angles, although the second derivatives at the minimum of the NNO–Ar surface give a reasonably good accounting of the force constants k_s and k_b derived from experimental centrifugal distortion constants.

[1] C. H. Joyner, T. A. Dixon, F. A. Baiocchi, and W. Klemperer, J. Chem. Phys. **75**, 5285 (1981).
[2] C. Dutton, A. Sazonov, and R. A. Beaudet, J. Phys. Chem. **100**, 17772 (1996).
[3] Y. J. Xu and A. R. W. McKellar, J. Mol. Spectrosc. **180**, 164 (1996).
[4] H. B. Qian and B. J. Howard, J. Mol. Spectrosc. **184**, 156 (1997).
[5] R. W. Randall, T. R. Dyke, and B. J. Howard, Faraday Discuss. Chem. Soc. **86**, 21 (1988).
[6] Y. P. Zeng, S. W. Sharpe, D. Reifschneider, C. Wittig, and R. A. Beaudet, J. Chem. Phys. **93**, 183 (1990).
[7] J. Hodge, G. D. Hayman, T. R. Dyke, and B. J. Howard, J. Chem. Soc., Faraday Trans. 2 **82**, 1137 (1986).
[8] T. A. Hu, E. L. Chappell, and S. W. Sharpe, J. Chem. Phys. **98**, 6162 (1993).
[9] B. J. Howard, in *Structure and Dynamics of Weakly Bonded Molecular Complexes*, edited by A. Weber, NATO ASI Series C, Vol. 212, (Reidel, Dordrecht, 1987), pp. 69–84.
[10] H. B. Qian, W. A. Herrebout, and B. J. Howard, Mol. Phys. **91**, 689 (1997).
[11] Z. S. Huang and R. E. Miller, J. Chem. Phys. **89**, 5408 (1988).
[12] D. J. Pauley, M. A. Roehig, L. Adamowicz, J. C. Shea, S. T. Haubrich, and S. G. Kukolich, J. Chem. Phys. **94**, 899 (1991).
[13] H. O. Leung, D. Gangwani, and J. U. Grabow, J. Mol. Spectrosc. **184**, 106 (1997).
[14] H. O. Leung, J. Chem. Phys. **108**, 3955 (1998).
[15] L. Berreby and E. Dayan, Mol. Phys. **48**, 581 (1983).
[16] C. Dreyfus and J. Cartigny, J. Chem. Phys. **80**, 5388 (1984).
[17] L. Berreby and E. Dayan, Chem. Phys. Lett. **243**, 85 (1995).
[18] C. Dreyfus, C. Breuillard, and Y. Guissani, Mol. Phys. **62**, 1275 (1987).
[19] H. W. Nicolaisen and H. Maeder, Mol. Phys. **73**, 349 (1991).
[20] C. J. Jameson, M. A. ter Horst, and A. K. Jameson, J. Chem. Phys. **109**, 10227 (1998), preceding paper.
[21] C. J. Jameson, A. K. Jameson, J. K. Hwang, and N. C. Smith, J. Chem. Phys. **89**, 5642 (1988).
[22] R. L. Armstrong, M. Bogdan, K. R. Jeffrey, C. Bissonnette, and F. R. W. McCourt, J. Chem. Phys. **99**, 5754 (1993).
[23] R. S. Wagner, R. L. Armstrong, C. Lemaire, and F. R. W. McCourt, J. Chem. Phys. **84**, 1137 (1986).
[24] C. Lemaire and R. L. Armstrong, Can. J. Phys. **63**, 179 (1985).
[25] L. Beneventi, P. Casavecchia, G. G. Volpi, C. C. K. Wong, and F. R. W. McCourt, J. Chem. Phys. **98**, 7926 (1993).
[26] M. A. ter Horst and C. J. Jameson, J. Chem. Phys. **105**, 6787 (1996).
[27] M. A. ter Horst and C. J. Jameson, J. Chem. Phys. **102**, 4431 (1995).
[28] F. R. W. McCourt, M. A. ter Horst, and C. J. Jameson, J. Chem. Phys. **102**, 5752 (1995).
[29] F. R. W. McCourt, J. J. M. Beenakker, W. E. Köhler, and I. Kuščer, *Nonequilibrium Phenomena in Polyatomic Gases Part I. The Dilute Gas* (Oxford University Press, Oxford, 1990), Vol. 1.
[30] F. R. W. McCourt, J. J. M. Beenakker, W. E. Köhler, and I. Kuščer, *Nonequilibrium Phenomena in Polyatomic Gases Part II. Cross Sections, Scattering and Rarefield Gases* (Oxford University Press, Oxford, 1990), Vol. 2.
[31] M. A. ter Horst, Ph.D. Thesis, University of Illinois at Chicago, 1994.
[32] J. Kestin and S. T. Ro, Ber. Bunsenges. Phys. Chem. **86**, 948 (1982).
[33] J. Kestin, H. E. Khalifa, S. T. Ro, and W. A. Wakeham, Physica A **88**, 242 (1977).
[34] C. Dreyfus, L. Berreby, and E. Dayan, Chem. Phys. Lett. **79**, 476 (1981).
[35] R. L. Armstrong, J. M. Blumenfeld, and C. G. Gray, Can. J. Phys. **46**, 1331 (1968).
[36] C. Dreyfus, D. Balou, and N. Brigot-Dutartre, J. Chem. Phys. **80**, 5393 (1984).
[37] C. J. Jameson and A. K. Jameson, J. Chem. Phys. **93**, 3237 (1990).
[38] J. B. Anderson, J. Chem. Phys. **63**, 1499 (1975).
[39] J. B. Anderson, J. Chem. Phys. **65**, 4121 (1976).
[40] V. Buch, J. Chem. Phys. **97**, 726 (1992).
[41] P. Sandler, J. O. Jung, M. M. Szczesniak, and V. Buch, J. Chem. Phys. **101**, 1378 (1994).
[42] K. A. Franken and C. E. Dykstra, Chem. Phys. Lett. **220**, 161 (1994).
[43] M. H. Kalos, Phys. Rev. A **2**, 250 (1970).
[44] B. J. Adler and D. M. Ceperley, J. Chem. Phys. **81**, 5833 (1984).
[45] M. A. Suhm and R. O. Watts, Phys. Rep. **204**, 293 (1991).
[46] A. C. de Dios and C. J. Jameson, J. Chem. Phys. **107**, 4253 (1997).